TWO-DIMENSIONAL FINITE DIFFERENCE BASED DATA-DRIVEN THERMAL MODELING OF IN-SITU AUTOMATED FIBER PLACEMENT

Allyson Fontes[1] and Farjad Shadmehri[2]

[1] Department of Mechanical, Industrial, and Aerospace Engineering, Concordia University, Montréal, Canada, allyson.fontes@concordia.ca
[2] Department of Mechanical, Industrial, and Aerospace Engineering, Concordia University, Montréal, Canada, farjad.shadmehri@concordia.ca

Keywords: Deep neural network, Automated fiber placement, Thermal modeling

ABSTRACT

The study aimed to develop a data-driven model to predict temperature history during in-situ consolidation of thermoplastic composites using Automated Fiber Placement (AFP). Temperature gradients produced during in-situ AFP processing are essential for determining residual stresses and deformation. Temperature curves were generated using a 2-dimensional finite-difference code developed by Tafreshi et al. (2019) for various combinations of Hot Gas Torch (HGT) temperatures and heat source velocity. Temperature curves for multiple locations through the thickness were extracted to develop the model. A feedforward neural network with four input features, three hidden layers, and one output was trained to predict the temperature distribution within the composite. The network's inputs were the heat source's position in the *x*-direction [m], the thermocouple location in the thickness (i.e., z-direction) [m], the HGT temperature [ºC], and the torch speed [m/s]. The network's output was the temperature at a location in the *x-z* domain for the given process conditions. A hyperparameter search was conducted for the number of hidden layers, units per hidden layer, and learning rate. A neural network with 256 units per hidden layer and a learning rate of 0.01 was found to have the best performance. A maximum prediction error of 2.70ºC (2.6%) was obtained on the training set, whereas a maximum prediction error of 9.44ºC (7.4%) was obtained on the test set. The research demonstrated that neural networks could simulate the thermal history developed during in-situ processing. The scope of future studies will be expanded to create a model using experimental data.

1 INTRODUCTION

The growing demand for composite materials in high-performance industries has led to the need for automated manufacturing processes that can provide increased throughput and repeatability. The in-situ manufacturing of thermoplastic composites using Automated Fiber Placement (AFP) is a technique that offers the potential for fast production and large-scale manufacturing of high-performance composite structures [1]. In-situ AFP of thermoplastics is an additive manufacturing process that eliminates the need for secondary thermal processing. During this process, tapes of thermoplastic composite are laid on a mandrel layer-by-layer, and a heat source locally melts the incoming tape before a consolidation roller applies pressure and bonds it to the composite substrate (Figure 1) [2], [3].

Hot Gas Torch (HGT) assisted in-situ AFP transfers heat to the incoming tape through forced convection. This process is modelled by Newton's law of cooling $\dot{q}=h_{HGT}\Delta T$ where $\dot{q}$ is the heat flux [W/m^2], h_{HGT} is the convective heat transfer coefficient [W/m^2K], and ΔT is the temperature differential between the two media [4]. Heat is also dissipated through the composite in all directions via heat conduction while the ambient air cools the exterior surfaces. However, due to the transient nature of this process, large thermal gradients develop in the composite substrate, resulting in residual stresses, deformation, and variations of crystalline regions [3], [5]. Therefore, the temperature history is the most critical parameter since it governs the consolidation behaviour (i.e., intimate contact and healing), crystallisation kinetics, and void dynamics [6]–[9].

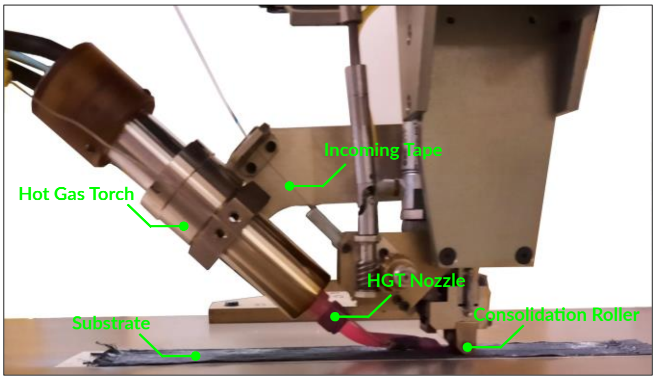

Figure 1. The AFP robot's head.

Numerical models that describe the heat transfer that occurs during in-situ AFP processing have been developed [10]–[13]. However, these models are computationally expensive because the whole domain must be simulated for each combination of the process parameters. Developing a data-driven model would reduce simulation times and allow for rapid iteration. This work aims to improve the prediction of the dynamic in-situ AFP manufacturing process by applying data-driven modeling to thermal history prediction. In this study, a two-dimensional (2D) data-driven thermal model of the in-situ AFP manufacturing of thermoplastics is developed on data from a Finite Difference (FD) model developed by Tafreshi et al. [14]. To the author's knowledge, this study marks the first time a Machine Learning (ML) based thermal model of the in-situ AFP manufacturing is developed. The methodology used to generate the data and to train the data-driven model is presented in detail. Future work will expand the methodology to the three-dimensional space using data from experimentally validated simulations and, eventually, experimental data.

2 FINITE DIFFERENCE MODEL

The following section summarizes the FD model used for data generation. The full details of the FD model implementation are described in [14]. In their work, Tafreshi et al. [14] developed a two-dimensional transient heat transfer model of the in-situ AFP process of carbon fiber/PEEK (AS4/APC-2 by Solvay). The authors developed a FD code of the transient heat transfer process in a rectangular domain consisting of a composite substrate and aluminium mandrel. The formulations for the interior and boundary nodes were developed by applying the energy balance to the discretised domain. Specifically, interior nodes were subjected to heat conduction in the *x*-direction and *z*-direction. The boundary nodes on the top surface were subjected to convective heat transfer due to the HGT or ambient air, depending on the location of the moving heat source. Nodes on the edges of the domain were subjected to ambient air throughout the process. The explicit method solved the transient heat transfer problem. A MATLAB (MathWorks Inc.) computer code was written for this purpose. The initial conditions and constant input parameters for the FD code are outlined in Table 1. Other input parameters, such as the heat source velocity (v_{HGT}), HGT convective heat transfer coefficient (h_{HGT}), and HGT temperature (T_{HGT}) were varied according to the AFP operating window. The material properties of the composite and mandrel are listed in [14].

3 DATA-DRIVEN HEAT TRANSFER MODEL

This section explains the steps to develop the 2-dimensional neural network model capable of predicting the temperature during the in-situ AFP process for various processing conditions. The steps to generate data and the methodology for training the neural network are outlined.

Metric	Value	Unit
Heated length	10	[mm]
Ambient and initial temperature	25	[°C]
Ambient air convective heat transfer coefficient (h_{air})	10	[W/m^2K]
Composite and mandrel length in *x*-direction	508	[mm]
Mesh size in *x*-direction	1	[mm]
Composite thickness in the *z*-direction	1.27 (i.e., ten layers)	[mm]
Mandrel thickness in the *z*-direction	10	[mm]
Composite mesh size in the *z*-direction	Three nodes per layer	-
Mandrel mesh in the *z*-direction	1	[mm]

Table 1. The FD code input parameters.

3.1 Data generation

Data was generated using Tafreshi et al.'s [14] FD model introduced in Section 2. Specifically, the data was produced with variable h_{HGT}, v_{HGT}, and T_{HGT} at one location in the layup direction (i.e., *x*-direction) and multiple locations in the thickness direction (i.e., *z*-direction). The FD model was iteratively run for T_{HGT} of 650, 725, 800, 875, and 950°C, and v_{HGT} of 50.8, 76.2, 101.6, 127, and 152.4 mm/s. The h_{HGT} is a function of the HGT process parameters, which vary for each iteration. The values for the h_{HGT} were approximated using the methodology proposed by Aghababaei Tafreshi et al. [15]. In their work, different values of the h_{HGT} were estimated using impinging jet theory. Specifically, the h_{HGT} coefficient for various T_{HGT}, gas flow rates (Q), nozzle and roller spacing (H) were identified. Full details on the methodology can be found in [15]. The h_{HGT} values for a Q of 90 standard litres per minute (SLPM) and H of 2.5 mm were taken from [15] for the data generation. The h_{HGT} values for T_{HGT} of 600, 700, 800, and 900°C are 572, 615, 669, and 727 W/m^2K, respectively. Using these points, the h_{HGT} coefficients for T_{HGT} of 650, 725, 875, and 950°C were linearly interpolated using a 1D interpolating spline. The SciPy Interpolated Univariate Spline fit [16] was used for this. The results of the interpolation are shown in Figure 2.

Using the obtained h_{HGT} coefficients, Tafreshi et al.'s [14] FD MATLAB model was run for the abovementioned combinations of the T_{HGT} and v_{HGT}. The temperature curves at the midpoint of the layup direction (i.e., 254 mm) were extracted from one to five layers below the torch (Figure 3). The data was then split into a train and test set, according to Figure 4. All layers at a given point were used for the training or testing. For instance, temperature curves for all layers with T_{HGT} of 650°C and v_{HGT} of 50.8 mm/s were used for training. Each temperature curve had 50,800 data points corresponding to the torch positions in the *x*-direction.

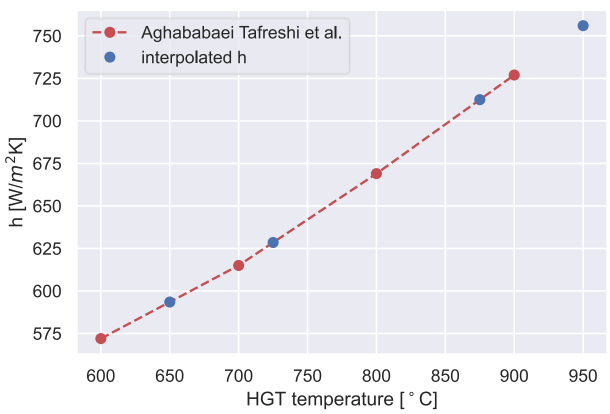

Figure 2. Interpolation of h_{HGT} coefficient from [15].

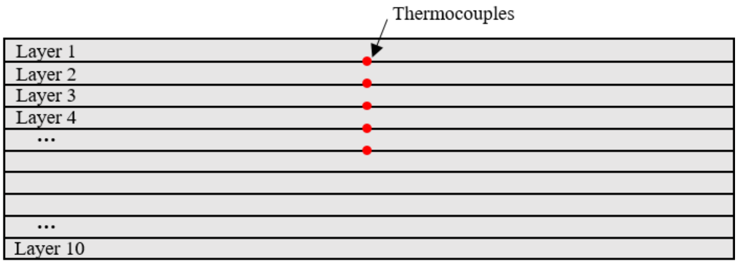

Figure 3. Schematic of the thermocouple locations through the thickness.

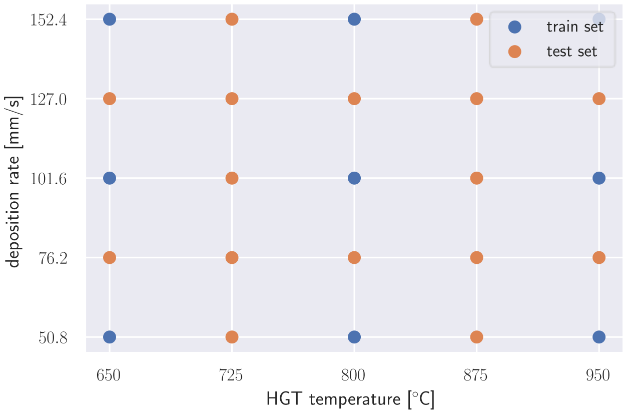

Figure 4. The train-test data split.

3.2 Neural network implementation

The following section outlines the inputs and outputs of the 2-dimensional thermal neural network model and the training process used for the model development.

3.2.1 Inputs and output

The goal of developing a 2-dimensional data-driven model is to predict the temperature distribution during in-situ AFP at various locations within the composite and for multiple combinations of the processing parameters. Therefore, the neural network must create a mapping from the domain and process conditions to the temperature distribution. The neural network's inputs were selected to be the heat source's position in the *x*-direction [m], the thermocouple's position with respect to the heat source in the thickness (i.e., *z*-direction) [m], the T_{HGT} [°C], and the v_{HGT} [m/s]. The gas flow rate (Q) and nozzle and roller spacing (H) were held constant, so they are excluded from the inputs. Since the T_{HGT} is magnitudes larger than the other three input features, it was normalized to be between 0 and 1 for improved training performance. The neural network's output is the temperature at the given point in the *x*-*z* domain for a given combination of the process parameters.

3.2.2 Neural network architecture and training

A neural network was developed using Python [17] and PyTorch, an open-source ML framework [18]. The Adaptive Moment Estimation (Adam) optimization algorithm was used for training. In addition, the mean squared error (MSE) loss function was selected to evaluate the networks' performance and compute the weight updates via backpropagation. The MSE loss function is defined as [19]

$$L(y_i, \hat{y}_i) = \frac{1}{N}\sum_{i=1}^{N}(y_i - \hat{y}_i)^2 \tag{1}$$

where N is the number of training data points in a mini-batch, y_i is the data's ground truth, and $\hat{y_i}$ is the network's prediction/output. A hyperparameter search was conducted for the learning rate, the number of hidden layers, and the number of units per layer. The Rectified Linear Unit (ReLU) activation function was maintained for all hidden layers, whereas linear activation was used for the output layer. Neural network architectures were trained with one to three hidden layers and 256 to 2048 units per hidden layer. Learning rate values from 10^{-1} to 10^{-4} were also tested. The learning rate of 0.01 was found to be ideal. The combination of hyperparameters that produced the lowest training loss was selected as the final model. Each model was trained for 2,000 epochs using mini-batches of 32,768 data points. Table 2 summarizes the network's best architecture and training method.

Metric	Value
Optimization algorithm	Adam
Hidden layer activation function	ReLU
Output layer activation function	Linear
Cost function	MSE
Number of hidden layers	3
Units per hidden layer	256
Learning rate (α)	0.01
Mini-batch size	32,768
Epochs	2,000

Table 2. The optimized neural network architecture and hyperparameters.

4 RESULTS AND DISCUSSION

The following section presents the neural network's predictions for both the training and test sets and evaluates its performance for process parameters beyond the range of the training data.

4.1 Neural network interpolation predictions

The neural net described in the previous section obtained an average MSE of 0.00065 on the individual temperature curves of the train set and 0.00198 on the test set curves. Moreover, the maximum error in temperature prediction within the train and test set were 2.70°C (2.6%) and 9.44°C (7.4%). Plots of the temperature prediction through the thickness for a T_{HGT} of 875°C and v_{HGT} of 50.8 mm/s are shown in Figure 5. The graph shows how the temperature varies through the composite thickness. The heating and cooling rates decrease as the distance between the heat source and thermocouple increases because the heat dissipates in all directions based on the material's conductivity. As seen in the figure, the shape of the temperature curve changes through the thickness. The neural network has difficulty learning the shape of the curve at the peaks. As a result, the network predicts sharp peaks for the next couple of layers below the torch, and the maximum error for each curve commonly occurs around the peak temperature. Nonetheless, the errors remain low and are negligible. More importantly, the neural network successfully captures the cooling rates. This is critical for predicting residual stresses and crystallinity within the final composite part.

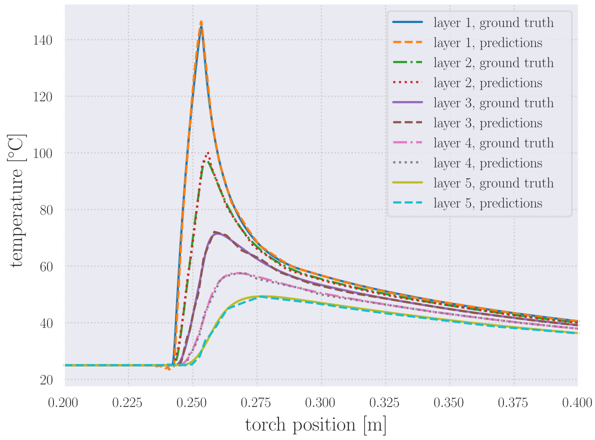

Figure 5. Neural network predictions through the thickness for T_{HGT}=875°C and v_{HGT}=50.8mm/s from the test set.

Next, the 2D temperature distributions obtained from the FD model are plotted alongside the neural network predicted distributions in Figure 6 and Figure 7. The distributions for when the heat source is midway through the layup direction are shown. The plots were generated for the combination of process parameters from the train and test sets with the highest predictive errors. The shape of the predicted temperature distributions through the thickness and the layup direction is consistent with the FD model. The neural network learned the overall trend in the temperature within the domain. A notable difference is that the equivalent temperature lines for the FD model are smooth, whereas the neural network's lines are jagged. This results from the abovementioned variation in the temperature peaks through the thickness.

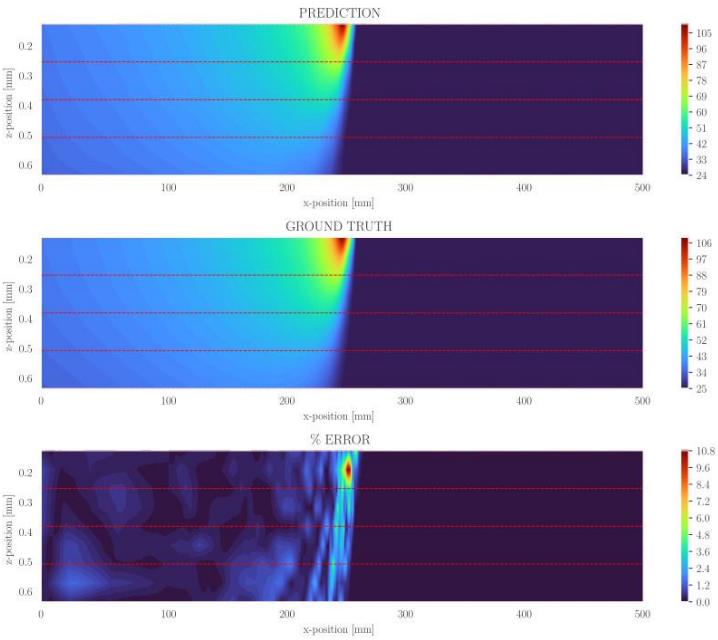

Figure 6. The 2D temperature distribution from the FD model and neural network for T_{HGT}=950°C and v_{HGT}= 101.6mm/s from the train set.

The neural network's 2D temperature distribution for data unseen during training is consistent with the ground truth (Figure 7). For this simulation, the maximum temperature outputted by the neural network for the first layer was 137.54°C, and the model's maximum was 128.31°C. The difference between these two peaks is also insignificant (7.2%). Overall, the neural network successfully captures the shape of the heat distribution despite having some slight local variations around the curve peaks.

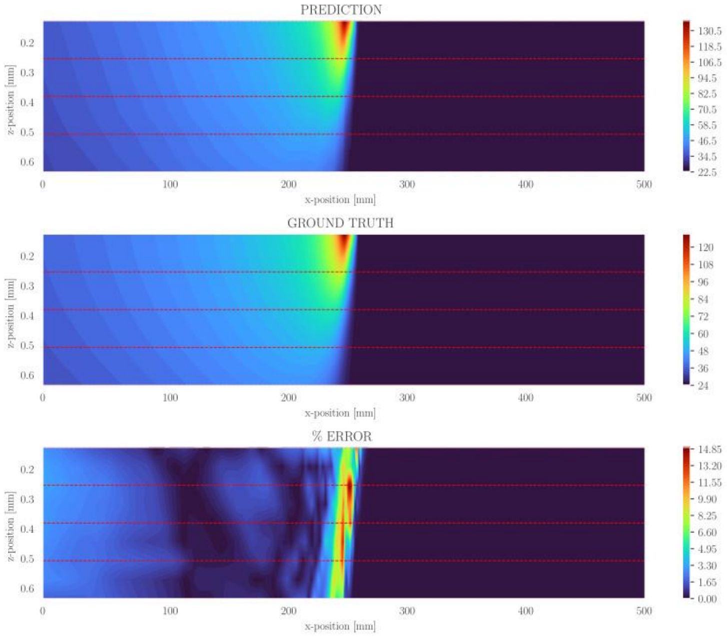

Figure 7. The 2D temperature distribution from the FD model and neural network for T_{HGT}=950°C and v_{HGT}=76.2mm/s from the test set.

4.2 Neural network extrapolation predictions

The neural network's ability to extrapolate outside the training and testing region was evaluated as a last step. Extrapolation of the HGT temperature and deposition rate was examined. Temperature distribution predictions for T_{HGT} of 600°C and 800°C with v_{HGT} of 50.8mm/s and 25.4 mm/s were generated. The predictions shown in Figure 8 reveal that the neural network struggled with extrapolating for the deposition rates. For deposition rates lower than those included in the training and testing sets, temperature errors of over 20°C were observed. However, the network was more robust in extrapolating the T_{HGT}, predicting maximum errors ranging from 5 to 10°C for T_{HGT} not contained within the train set. While the neural network demonstrated promising extrapolation capabilities for T_{HGT}, it showed limitations in extrapolating v_{HGT}. For practical applications, training the neural network on the lower and upper limits of the processing range would be ideal for eliminating the need for extrapolation.

5 CONCLUSIONS

This work proposes and develops a data-driven thermal model of the in-situ AFP process. The data-driven model was developed using data from a 2-dimensional FD thermal model developed by Tafreshi et al. [14]. The model accurately predicts the thermal history for various combinations of the T_{HGT} and v_{HGT}. As expected, the thermal model's predictions for interpolation situations outperform the extrapolation cases. For optimal performance, the model should train on the upper and lower limits of the process parameters. This data-driven approach provides a path for online prediction and real-time control of the in-situ AFP process. Future studies will incorporate data from experiments or experimentally validated simulations for temperature prediction in 3-dimensional space.

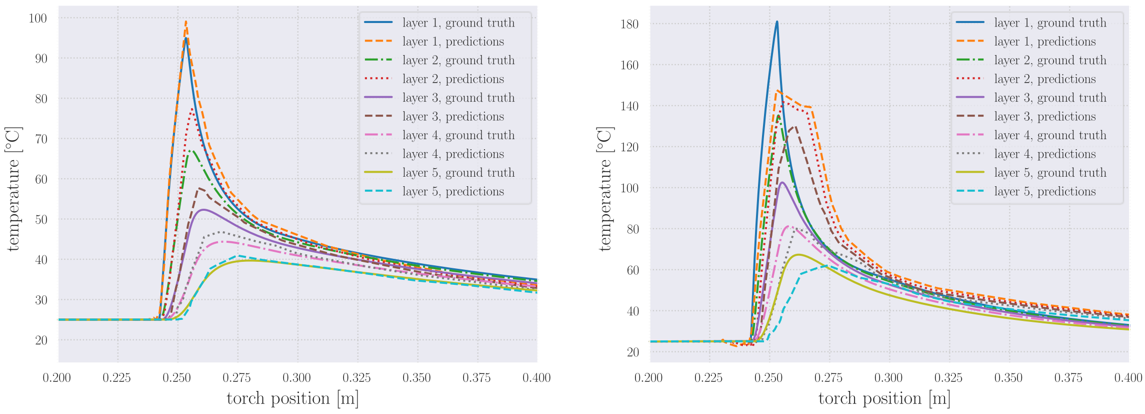

Figure 8. Extrapolation results for T_{HGT}=600°C and v_{HGT}=50.8mm/s (left) and T_{HGT}=800°C and v_{HGT}=25.4mm/s (right).

REFERENCES

[1] C. Grant, Automated processes for composite aircraft structure, *Industrial Robot: An International Journal*, **33**, 2006, pp. 117–121 (doi: 10.1108/01439910610651428).

[2] S. V. Hoa, *Principles of the Manufacturing of Composite Materials*, 2nd ed., Lancaster, PA: DEStech Publications, Inc., 2018.

[3] S. Van Hoa, M. Duc Hoang, and J. Simpson, Manufacturing procedure to make flat thermoplastic composite laminates by automated fibre placement and their mechanical properties, *Journal of Thermoplastic Composite Materials*, **30**, 2017, pp. 1693–1712 (doi: 10.1177/0892705716662516).

[4] Y. A. Çengel and A. J. Ghajar, *Heat and mass transfer : fundamentals & applications*, Sixth ed., New York, NY: McGraw-Hill Education, 2020.

[5] F. O. Sonmez, H. T. Hahn, and M. Akbulut, Analysis of Process-Induced Residual Stresses in Tape Placement, *Journal of Thermoplastic Composite Materials*, **15**, 2002, pp. 525–544, (doi: 10.1177/0892705702015006207).

[6] C. R. Choe and K. H. Lee, Nonisothermal Crystallization Kinetics of Poly(etheretherketone) (PEEK), *Polymer Engineering & Science*, **29**, 1989, pp. 801–805.

[7] J. Tierney and J. W. Gillespie, Modeling of In Situ Strength Development for the Thermoplastic Composite Tow Placement Process, *Journal of Composite Materials*, **40**, 2006, pp. 1487–1506 (doi: 10.1177/0021998306060162).

[8] A. Brasington, C. Sacco, J. Halbritter, R. Wehbe, and R. Harik, Automated fiber placement: A review of history, current technologies, and future paths forward, *Composites Part C: Open Access*, **6**, 2021, p. 100182 (doi: 10.1016/j.jcomc.2021.100182).

[9] A. Khodaei and F. Shadmehri, Intimate contact development for automated fiber placement of thermoplastic composites, *Composites Part C: Open Access*, **8**, 2022, p. 100290 (doi: 10.1016/j.jcomc.2022.100290).

[10] H. J. Kim, S. K. Kim, and W. I. Lee, A study on heat transfer during thermoplastic composite tape lay-up process, *Experimental Thermal and Fluid Science*, **13**, 1996, pp. 408–418 (doi: 10.1016/S0894-1777(96)00095-7).

[11] C. M. Stokes-Griffin, P. Compston, T. I. Matuszyk, and M. J. Cardew-Hall, Thermal modelling of the laser-assisted thermoplastic tape placement process, *Journal of Thermoplastic Composite Materials*, **28**, 2013, pp. 1445–1462 (doi: 10.1177/0892705713513285).

[12] Z. Li, T. Yang, and Y. Du, Dynamic finite element simulation and transient temperature field analysis in thermoplastic composite tape lay-up process, *Journal of Thermoplastic Composite Materials*, **28**, 2015, pp. 558–573 (doi: 10.1177/0892705713486135).

[13] L. Zacherl, F. Shadmehri, and K. Rother, Determination of convective heat transfer coefficient for hot gas torch (HGT)-assisted automated fiber placement (AFP) for thermoplastic composites,

Journal of Thermoplastic Composite Materials, 2021, p. 0892705720982363 (doi: 10.1177/0892705720982363).

[14] O. A. Tafreshi, S. V. Hoa, F. Shadmehri, D. M. Hoang, and D. Rosca, Heat transfer analysis of automated fiber placement of thermoplastic composites using a hot gas torch, *Advanced Manufacturing: Polymer & Composites Science*, **5**, 2019, pp. 206–223 (doi: 10.1080/20550340.2019.1686820).

[15] O. Aghababaei Tafreshi, S. Van Hoa, F. Shadmehri, D. M. Hoang, and D. Rosca, Determination of convective heat transfer coefficient for automated fiber placement (AFP) for thermoplastic composites using hot gas torch, *Advanced Manufacturing: Polymer & Composites Science*, **6**, 2020, pp. 86–100 (doi: 10.1080/20550340.2020.1764236).

[16] P. Virtanen *et al.*, SciPy 1.0: Fundamental Algorithms for Scientific Computing in Python, *Nature Methods*, **17**, 2020, pp. 261–272 (doi: 10.1038/s41592-019-0686-2).

[17] "Python." Python Software Foundation, 2018. [Online]. Available: http://www.python.org

[18] A. Paszke *et al.*, "PyTorch: An Imperative Style, High-Performance Deep Learning Library," in *Advances in Neural Information Processing Systems 32*, H. Wallach, H. Larochelle, A. Beygelzimer, F. d'Alché-Buc, E. Fox, and R. Garnett, Eds., Curran Associates, Inc., 2019, pp. 8024–8035. [Online]. Available: http://papers.neurips.cc/paper/9015-pytorch-an-imperative-style-high-performance-deep-learning-library.pdf

[19] I. Goodfellow, Y. Bengio, and A. Courville, *Deep learning*. in Adaptive computation and machine learning. Cambridge, Massachusetts: The MIT Press, 2016. [Online]. Available: http://www.deeplearningbook.org/